J|A|C|S ARTICLES

Published on Web 07/07/2009

Metal−Organic Frameworks Impregnated with Magnesium-Decorated Fullerenes for Methane and Hydrogen Storage

Aaron W. Thornton,*[,†,‡] Kate M. Nairn,[†] James M. Hill,[‡] Anita J. Hill,[†] and Matthew R. Hill*[,†,§]

CSIRO Materials Science and Engineering, Private Bag 33, Clayton South MDC, Victoria 3169, Australia, Nanomechanics Group, School of Mathematics and Applied Statistics, University of Wollongong, Wollongong, NSW 2522, Australia, and School of Chemistry, University of Melbourne, Victoria 3010, Australia

Received January 5, 2009; Revised Manuscript Received May 5, 2009; E-mail: aaron.thornton@csiro.au; matthew.hill@csiro.au

Abstract: A new concept is described for methane and hydrogen storage materials involving the incorporation of magnesium-decorated fullerenes within metal−organic frameworks (MOFs). The system is modeled using a novel approach underpinned by surface potential energies developed from Lennard-Jones parameters. Impregnation of MOF pores with magnesium-decorated $Mg_{10}C_{60}$ fullerenes, denoted as **Mg−C$_{60}$@MOF**, places exposed metal sites with high heats of gas adsorption into intimate contact with large surface area MOF structures. Perhaps surprisingly, given the void space occupied by C_{60}, this impregnation delivers remarkable gas uptake, according to our modeling, which predicts exceptional performance for the **Mg−C$_{60}$@MOF** family of materials. These predictions include a volumetric methane uptake of 265 v/v, the highest reported value for any material, which significantly exceeds the U.S. Department of Energy target of 180 v/v. We also predict a very high hydrogen adsorption enthalpy of 11 kJ mol^{-1} with relatively little decrease as a function of H_2 filling. This value is close to the calculated optimum value of 15.1 kJ mol^{-1} and is achieved concurrently with saturation hydrogen uptake in large amounts at pressures under 10 atm.

Introduction

Metal−organic frameworks (MOFs) are the major candidates that might meet the U.S. Department of Energy (DoE) requirements for vehicular gas storage.[1] They possess intrinsically high surface areas and internal volumes, and these factors are useful for gas storage at high pressures and/or at low temperatures.[2] However, these operating conditions will most likely require heavy and potentially expensive system components for implementation, particularly within hydrogen-powered vehicles.[3] MOFs also show promising potential for methane storage, but further development of MOFs could lead to significant enhancements for the storage of both gaseous fuels.

Any materials that might store hydrogen at near-to-ambient conditions are highly sought after. However, to realize these operating conditions, the heat of adsorption for potential MOF (i.e., coordination polymer)[4] hydrogen sorbents must be drastically increased to around 15.1 kJ mol^{-1},[2,5,6] as this is the dominant factor for adsorption capacity at low pressures.[2] The heat of adsorption for hydrogen within MOFs is generally around 5−7 kJ mol^{-1}, but it has been reported as high as 13.5 kJ mol^{-1} for the first hydrogen atoms adsorbed.[5,7] The various approaches employed have included the functionalization of the organic ligands within the framework,[8] exposure of metal sites,[9,10] the use of narrow "slit" pores where the pore wall surface energy potentials may overlap,[11] and incorporation of Li clusters within MOF frameworks.[12]

The adsorption of methane within porous materials has recently attracted interest because of the need for an alternative to compressed natural gas powered vehicles, which operate at 205 atm and require complex and energy expensive multistage

[†] CSIRO Materials Science and Engineering.
[‡] University of Wollongong.
[§] University of Melbourne.

(1) Multi-Year Research, Development and Demonstration Plan: Planned Program Activities for 2003−2010; Technical Plan−Storage; U.S. Department of Energy; http://www1.eere.energy.gov/hydrogenandfuelcells/mypp/pdfs/storage.pdf.
(2) Frost, H.; Duren, T.; Snurr, R. Q. *J. Phys. Chem. B* **2006**, *110* (19), 9565.
(3) Rand, D. A. J.; Dell, R. M. *Hydrogen Energy: Challenges and Prospects*; Royal Society of Chemistry: Cambridge, UK, 2008.
(4) Batten, S. R.; Neville, S. M.; Turner, D. R. *Coordination Polymers: Design, Analysis and Application*; Royal Society of Chemistry: Cambridge, UK, 2008.
(5) Bhatia, S. K.; Myers, A. L. *Langmuir* **2006**, *22* (4), 1688.
(6) Menon, P. G. *Chem. Rev.* **1968**, *68* (3), 277.
(7) Vitillo, J. G.; Regli, L.; Chavan, S.; Ricchiardi, G.; Spoto, G.; Dietzel, P. D. C.; Bordiga, S.; Zecchina, A. *J. Am. Chem. Soc.* **2008**, *130* (26), 8386.
(8) Rowsell, J. L. C.; Yaghi, O. M. *J. Am. Chem. Soc.* **2006**, *128* (4), 1304.
(9) Dinca, M.; Dailly, A.; Liu, Y.; Brown, C. M.; Neumann, D. A.; Long, J. R. *J. Am. Chem. Soc.* **2006**, *128* (51), 16876.
(10) Dinca, M.; Long, J. R. *J. Am. Chem. Soc.* **2005**, *127* (26), 9376.
(11) Rzepka, M.; Lamp, P.; de la Casa-Lillo, M. A. *J. Phys. Chem. B* **1998**, *102* (52), 10894.
(12) Blomqvist, A.; Araujo, C. M.; Srepusharawoot, P.; Ahuja, R. *Proc. Natl. Acad. Sci. U.S.A.* **2007**, *104* (51), 20173.

10.1021/ja9036302 CCC: $40.75

compression equipment.[13] The U.S. DoE stipulates methane adsorption of 180 v/v at 298 K and 35 atm as the benchmark for adsorbed natural gas technology,[14] and the optimum adsorption heat has been calculated at 18.8 kJ mol^{-1}.[5] Most of the recent research effort in methane storage materials has focused on the development of porous carbons. However, even the most sophisticated carbon structures struggle to significantly surpass the 180 v/v target,[14−16] largely because of the inherently low adsorption heat for methane within carbons, typically around 10−15 kJ mol^{-1}.[13] However, primarily because of the higher adsorption heats inherent to them, MOFs exhibit superior performance[17,18] and exceed the DoE target with the highest reported value currently 230 v/v.[19]

Light metal hydrides[20,21] possess adsorption heats well above the optimum calculated value for hydrogen storage.[5,22] Consequently, metal hydrides require around 300 °C for desorption. The pyrophoric nature and inefficient cyclability of these materials are further drawbacks to their use as monolithic storage materials, but they have potential as components of composite materials, in particular where they emulate exposed metal sites, sought after as high enthalpy hydrogen sorption locations in MOFs.

Fullerenes are particularly attractive candidates as components for hydrogen storage materials.[23] As recently shown in the literature, C_{60} fullerenes may store up to 58 hydrogen atoms internally without destroying the fullerene structure,[24] which is equivalent to an uptake of 7.5 wt %. In addition, it has been established that decoration of the external fullerene surface with transition metals dramatically enhances their surface adsorption performance in comparison to bare fullerenes, potentially yielding an additional 8 wt % hydrogen uptake on the external surface through Kubas interaction,[25] or up to 60 H_2 molecules per fullerene in the case of Li decoration.[26] The hydrophobic nature of fullerenes also makes them suitable candidates for methane storage.

Given that MOFs, exposed metal sites (for example, light metal hydrides), and fullerenes each hold potential for gas storage, a material that has the combined attributes of each of these systems is particularly desirable. Here we propose and model a material combining all of these components. On the basis of the impregnation concept[27] first demonstrated by Chae et al.,[28] who show that C_{60} fullerenes readily impregnate the porous network of MOF-177 (denoted by **C_{60}@MOF**), we predict that the magnesium-decorated $Mg_{10}C_{60}$ within similar structures (denoted as **Mg−C_{60}@MOF**) should deliver a very high gas storage enhancement. The proposed material is shown schematically in Figure 1.

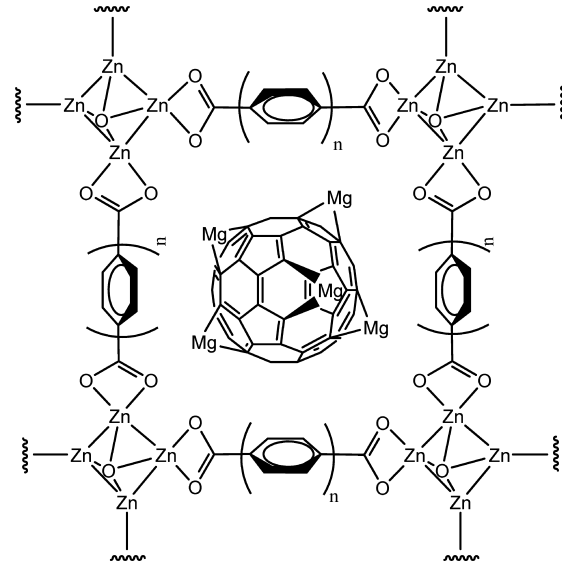

Figure 1. Schematic representation for proposed material **Mg−C_{60}@MOF** showing a MOF cavity impregnated with magnesium-decorated C_{60}.

Adsorption has been successfully simulated previously using the Lennard-Jones potential function and a variety of Monte Carlo techniques.[2,30−33] Here we use the Lennard-Jones potential and assume a spherical geometry for the framework cavities to analytically evaluate the adsorption heat, weight percentage, and volumetric hydrogen (and methane) uptake assuming variable cavity size and fullerene impregnation. This novel method (topologically integrated mathematical thermodynamic adsorption model, TIMTAM) is shown to reproduce the main features of experimental isotherms, without the need to run computationally expensive simulations, and hence may be used to predict the effects of cavity size and fullerene impregnation on the adsorption heats and the gas uptake. The results obtained using **Mg−C_{60}@MOF** for the TIMTAM approach show large hydrogen uptake capacities at low pressures, which are achieved with one of the highest heats of adsorption for a physisorption-based storage material. Methane volumetric uptakes at 298 K/35 atm are also predicted to be the highest reported values for any material.

Methods

The MOF cavity structure is approximated to enable the development of a potential energy function, which is then used to predict various important adsorption results such as the average potential energy for adsorption, volume free for adsorption, heat of adsorption, and adsorbate uptake. A similar

(13) Menon, V. C.; Komarneni, S. *J. Porous Mater.* **1998**, *5* (1), 43.
(14) Burchell, T.; Rogers, M. *SAE Tech. Pap. Ser.* **2000**, 2000−01−2205.
(15) Lozano-Castello, D.; Alcaniz-Monge, J.; de la Casa-Lillo, M. A.; Cazorla-Amoros, D.; Linares-Solano, A. *Fuel* **2002**, *81* (14), 1777.
(16) Celzard, A.; Fierro, V. *Energy Fuels* **2005**, *19* (2), 573.
(17) Eddaoudi, M.; Kim, J.; Rosi, N.; Vodak, D.; Wachter, J.; O'Keeffe, M.; Yaghi, O. M. *Science* **2002**, *295* (5554), 469.
(18) Wang, X.-S.; Ma, S.; Rauch, K.; Simmons, J. M.; Yuan, D.; Wang, X.; Yildirim, T.; Cole, W. C.; Lopez, J. J.; de Meijere, A.; Zhou, H.-C. *Chem. Mater.* **2008**, *20* (9), 3145.
(19) Ma, S.; Sun, D.; Simmons, J. M.; Collier, C. D.; Yuan, D.; Zhou, H.-C. *J. Am. Chem. Soc.* **2008**, *130* (3), 1012.
(20) Gray, E. M. *Adv. Appl. Ceram.* **2007**, *106* (1−2), 25.
(21) Sudik, A.; Yang, J.; Halliday, D.; Wolverton, C. *J. Phys. Chem. C* **2008**, *112* (11), 4384.
(22) See ref 6.
(23) Strobel, R.; Garche, J.; Moseley, P. T.; Jorissen, L.; Wolf, G. *J. Power Sources* **2006**, *159* (2), 781.
(24) Pupysheva, O. V.; Farajian, A. A.; Yakobson, B. I. *Nano Lett.* **2008**, *8* (3), 767.
(25) Yildirim, T.; Iniguez, J.; Ciraci, S. *Phys. Rev. B* **2005**, *72* (15), 153403.
(26) Sun, Q.; Jena, P.; Wang, Q.; Marquez, M. *J. Am. Chem. Soc.* **2006**, *128* (30), 9741.
(27) Rowsell, J. L. C.; Yaghi, O. M. *Angew. Chem., Int. Ed.* **2005**, *44* (30), 4670.
(28) Chae, H. K.; Siberio-Perez, D. Y.; Kim, J.; Go, Y.; Eddaoudi, M.; Matzger, A. J.; O'Keeffe, M.; Yaghi, O. M. *Nature* **2004**, *427* (6974), 523.
(29) Cox, B. J.; Hill, J. M. *J. Phys. A: Math. Theor.* **2008**, *41* (12), 125203.
(30) de Lange, R. S. A.; Keizer, K.; Burggraaf, A. J. *J. Membr. Sci.* **1995**, *104* (1−2), 81.
(31) Thornton, A. W.; Hilder, T.; Hill, A. J.; Hill, J. M. *J. Membr. Sci.* **2009**, *336* (1), 101.
(32) Cox, B. J.; Thamwattana, N.; Hill, J. M. *Proc. R. Soc. A* **2007**, *463* (2078), 461.
(33) Mayo, S. L.; Olafson, B. D.; Goddard, W. A. *J. Phys. Chem.* **1990**, *94* (26), 8897.

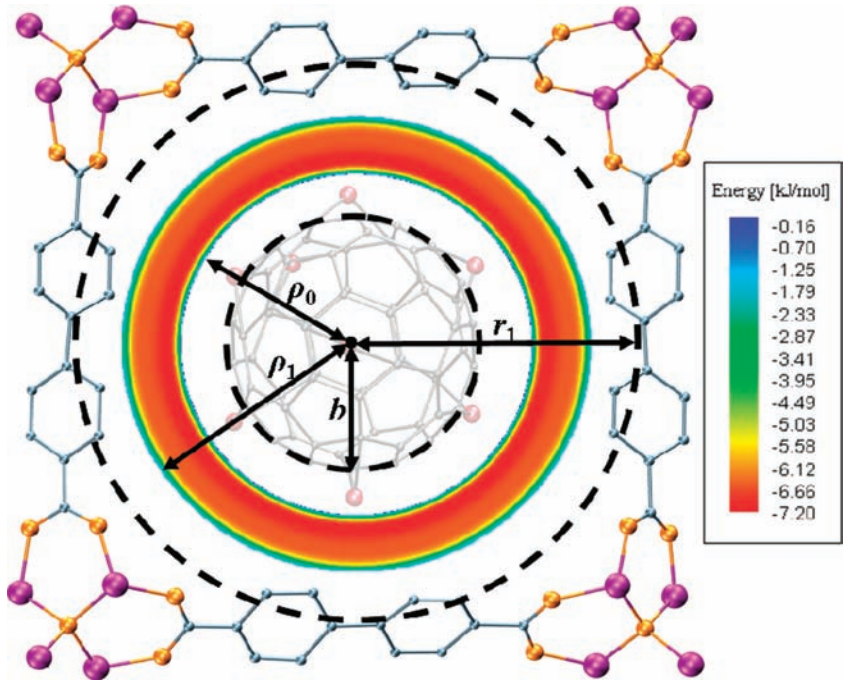

Figure 2. Potential energy for adsorption within the free volume of **Mg−C_{60}@MOF**.

approach was used previously to explore the optimization of porosity and chemistry for material performance, including successful determination of the adsorption of fullerenes onto the inside wall of carbon nanotubes[29] and the gas separation regimes within cylindrical pore channels.[30,31]

The TIMTAM approach taken here is an approximation that begins by assuming that the isoreticular MOF (IRMOF) structure is composed of spherically shaped cavities such that the cavity surface, defined at radius r_1, consists of the framework atoms, namely zinc, oxygen, carbon, and hydrogen, which we index $i = 1, 2, 3, 4$, respectively. These atoms are averaged over the cavity surface, creating a homogeneous layer onto which a gas molecule can adsorb. This approximation enables the development of a potential energy function between a gas molecule and the cavity surface based on the following 6−12 Lennard-Jones potential assuming a spherical geometry:

$$PE_{\mathrm{MOF}}(\rho) = \sum_{i=1}^{4}(-E_{6,i} + E_{12,i}) \tag{1}$$

$$E_{n,i} = \frac{2C_{n,i}\eta_i\pi r_1}{\rho(2-n)}\left(\frac{1}{(\rho + r_1)^{n-2}} - \frac{1}{(\rho - r_1)^{n-2}}\right) \tag{2}$$

where $C_{n,i} = 4\varepsilon_i\sigma_i^n$; ε_i and σ_i are the well depth and the kinetic diameter, respectively, found by using the Berthelot-Lorentz mixing rules between the gas molecule and atom i on the cavity surface. Further, η_i is the atomic surface density of atom i within the cavity surface at radius r_1 (Figure 2), and ρ is the distance between the gas molecule and the center of the cavity. For further details of the derivation of eqs 1 and 2, we refer the reader to Cox et al.[32] Dreiding[33] force field values are used for the framework atoms, and experimentally determined values are used for hydrogen[34] and methane.[35] Full details of the parameter values derived and employed for the TIMTAM method are included in Tables S1−S4 of the Supporting Information.

The effect of the insertion of decorated C_{60} fullerenes into the MOF cavity can be studied by including the potential energy of the interaction between the gas molecule and the surface of the fullerene. The interaction between an atom and a fullerene was formulated by Cox et al.[32] Here we extend this formulation to consider fullerenes that are functionalized with magnesium atoms, where we have chosen functionalization by 10 magnesium atoms, which is equal to the number of phenanthrene subunit bridging sites. The van der Waals interaction energy becomes

$$PE_{\mathrm{Mg_{10}C_{60}}}(\rho) = \sum_{j=1}^{2}(-E_{6,j} + E_{12,j}) \tag{3}$$

$$E_{n,j} = \frac{2C_{n,j}\eta_j\pi b}{\rho(2-n)}\left(\frac{1}{(\rho + b)^{n-2}} - \frac{1}{(\rho - b)^{n-2}}\right) \tag{4}$$

where $C_{n,j} = 4\varepsilon_j\sigma_j^n$, b is the radius of a fullerene, and here $j = 1, 2$ represents carbon and magnesium, respectively. By assuming that the fullerene is located in the center of the cavity, a combination of both expressions ($PE(\rho) = PE_{\mathrm{MOF}}(\rho) + PE_{\mathrm{Mg_{10}C_{60}}}(\rho)$) enables a prediction of the potential energy distribution throughout the cavity. For undecorated fullerenes, we simply omit the terms corresponding to $j = 2$.

In reality, the fullerenes will be randomly distributed throughout the porous network as demonstrated in recent molecular simulation work,[36] and therefore the assumption that the fullerenes are centrally located reflects the overall average behavior. The center of the cavity is the optimal position for the fullerene to deliver maximum gas adsorption; however, we demonstrated that the uptake results are still enhanced if the fullerene is positioned anywhere on the surface of the MOF

(34) Michels, A.; de Graaff, W.; Ten Seldam, C. A. *Physica* **1960**, *26* (6), 393.
(35) Maitland, G. C.; Rigby, M.; Smith, E. B.; Wakeham, W. A. *Intermolecular Forces: Their Origin and Determination*; Clarendon Press: Oxford, UK, 1981.
(36) Han, S. S.; Mendoza-Cortes, J. L.; Goddard, W. A., III. *Chem. Soc. Rev.* **2009**, *38* (5), 1460.

Table 1. Parameter Values for α and Cavity Radius r_1 Found from Fits to Experimental and Simulation Results, with ρ_1 Calculated so that $PE(\rho_1) = 0$[a]

exptl and sim results	α (fitted)	r_1 (Å) (fitted)	ρ_1 (Å) (calcd)	r^* (Å) (fixed)	$r_1 = (3/2)^{1/2}r^*$ (Å) (approximation)
Panella et al.[38] IRMOF-1	0.43	11.45	8.70	9.25	11.32
Ryan et al.[39] IRMOF-1	0.28	10.78	8.03	9.25	11.32
Kaye et al.[40] IRMOF-1	0.28	10.78	8.03	9.25	11.32
Frost et al.[2] IRMOF-8	0.28	12.74	10.00	10.70	13.10
Ryan et al.[39] IRMOF-10	0.28	14.45	11.70	12.25	15.00
Ryan et al.[39] IRMOF-16	0.28	18.25	15.50	14.40	17.64

[a] Fixed cavity radius r^* from Eddaoudi et al.[41] and cavity radius approximation $r_1 = (3/2)^{1/2}r^*$.

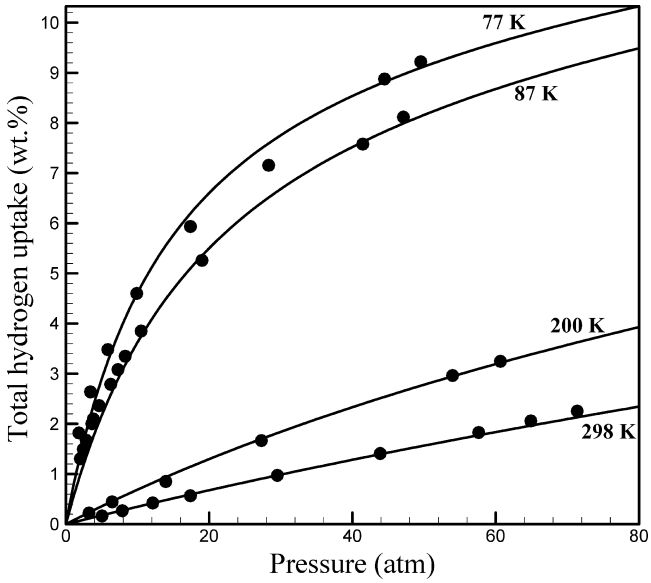

Figure 3. TIMTAM fit (solid lines) to Panella et al.[38] experimental results (●) for total hydrogen uptake by IRMOF-1 at 77, 87, 200, and 298 K. Panella et al.[38] measure the excess number of adsorbed molecules, reported as a quantity N_{ex} which was converted to total (absolute) adsorption n by the formula $n = N_{ex} + V_f \rho_g$, where ρ_g is the bulk gas density.[42]

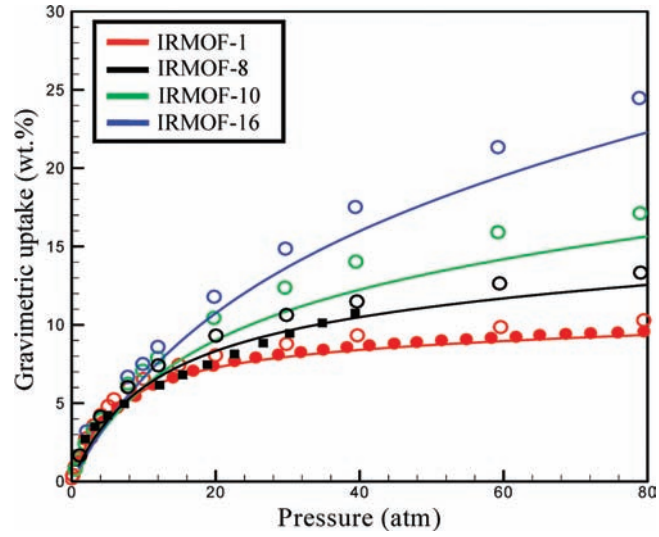

Figure 4. TIMTAM fit (solid lines) for total hydrogen uptake to experimental results for IRMOF-1[40] (●) and IRMOF-8[43] (■), Monte Carlo simulation results (○) for IRMOF-1, -10, -16,[39] and -8[2] at 77 K. Average systematic deviation ≈ 9%.

cavity wall (Figure S1 in the Supporting Information). This effect is confirmed by the recent uptake results determined by Monte Carlo methods[36] for MOF-177 impregnated with fullerenes.

If the kinetic energy of the gas molecule, $|KE|$, is less than the potential energy of the interaction between the gas molecule and the framework, $|PE|$, then the gas molecule will be adsorbed. Conversely, if $|KE| > |PE|$ the gas molecule will remain in the bulk phase. Hence, the probability of the molecule remaining as bulk gas is given by $\exp[-|PE|/RT]$ and the probability of the gas molecule adsorbing is given by $1 - \exp[-|PE|/RT]$. The cavity-free volume may then be split into two: the volume in which gas molecules are adsorbed

$$V_{ad} = \int_{\rho_0}^{\rho_1} 4\pi\rho^2\{1 - \exp[-|PE(\rho)|/RT]\}\, d\rho \qquad (5)$$

and that in which they remain as bulk gas

$$V_{bulk} = \int_{\rho_0}^{\rho_1} 4\pi\rho^2\{\exp[-|PE(\rho)|/RT]\}\, d\rho \qquad (6)$$

where R is the universal gas constant and T is the temperature (K). There are various ways of defining the total cavity-free volume, and here we define it as the total space within the cavity for which the potential energy is negative. The radial boundaries of this space are indicated by ρ_0 and ρ_1 in Figures 2 and 5A, where ρ_0 is equal to zero in the absence of a fullerene. An alternative definition of the total cavity-free volume could be the total space within the cavity for which the potential energy is less than the average kinetic energy of the bulk gas-phase RT. In this case, ρ_0 and ρ_1 would be temperature-dependent, satisfying $PE(\rho_0) = PE(\rho_1) = RT$. In this work, we use the former definition where ρ_0 and ρ_1 are independent of temperature; however, calculations show that the latter definition determines a total cavity-free volume increase of 3.5% at a temperature of 298 K, although this only results in a hydrogen uptake increase of 0.01 wt %. We note that the total cavity-free volume is equal to the sum of the volume free for adsorption and the volume free for bulk gas ($V_f = V_{ad} + V_{bulk}$). We believe that these expressions are crucial to determining adsorption performance, since the adsorbate is stored more densely in the adsorbed state than in the bulk gas state. The total number of molecules absorbed by the MOF at specified temperature and pressure is found by combining eqs 5 and 6 with the corresponding equations of state for adsorbed phase and bulk gas phase, respectively. Further details are provided in equations S2 and S3 of the Supporting Information.

Results and Discussion

In the modeling of the likely gas storage performance for our proposed material, it is crucial that the modeling output be verified against other experimental and simulation results to provide confidence in the accuracy of the predictions made. The difficulty of the sample preparation and measurement has led to varying reported experimental results, and simulation results also vary according to the different methods and the different parameter values adopted.[37] Therefore, we selected a sample

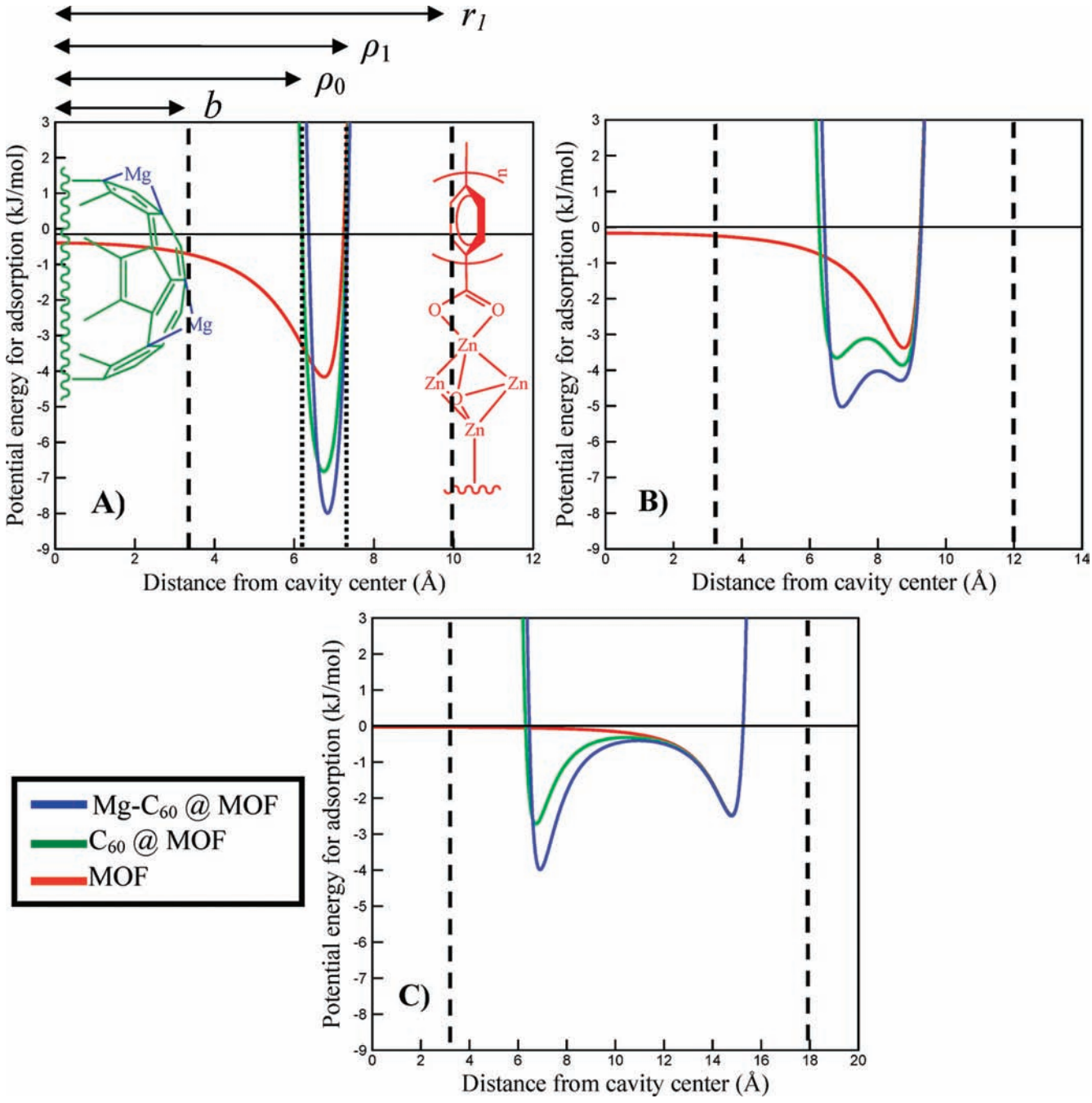

Figure 5. Profile of potential energy for adsorption within MOFs with cavity radii r_1 of (A) 10, (B) 12, and (C) 18 Å. Unfilled MOF (red), **C_{60}@MOF** (green), and **Mg_{10}-C_{60}@MOF** (blue). Cavity surface at radius r_1, fullerene surface at radius b, and free volume boundaries at ρ_0 and ρ_1 for **Mg−C_{60}@MOF** are labeled in Figure 5A for clarity.

set consisting of conservative uptake values[2,38−40] and used this set to calculate the empirical constant α, in equation S2 of the Supporting Information. Consequently, the empirical constant α is set to 0.35 (Figures 3 and 4 and Table 1). In addition, it is found that a good approximation for the cavity radius is $r_1 = (3/2)^{1/2}r^*$, where r^* is the fixed radius determined by Eddaoudi et al.[41] which represents the radius of the largest van der Waals sphere that fits into the cavity without touching the framework atoms. These particular experimental and simulation results are chosen for model validation since the data available encompass a wide range of temperatures, pressures, and cavity sizes. The model accurately portrays the observed effects of temperature, pressure, and cavity size on the adsorbate uptake and is consequently capable of predicting the effect of impregnated fullerenes within the MOF structure.

One of the major benefits expected from the impregnation of MOF structures is the surface potential energy overlap from the fullerene "guest" with that of the MOF "host" across the remaining free volume. This overlap could increase both the adsorption strength and the total amount of gas that is adsorbed in a dense fashion, as opposed to simply filling the pores in a lower density gaseous form. Figure 5 demonstrates these effects in three discrete cases, by varying r_1, the MOF cavity radius at which the framework atoms are approximately located.

(37) Thomas, K. M. *Dalton Trans.* **2009**, (9), 1487.

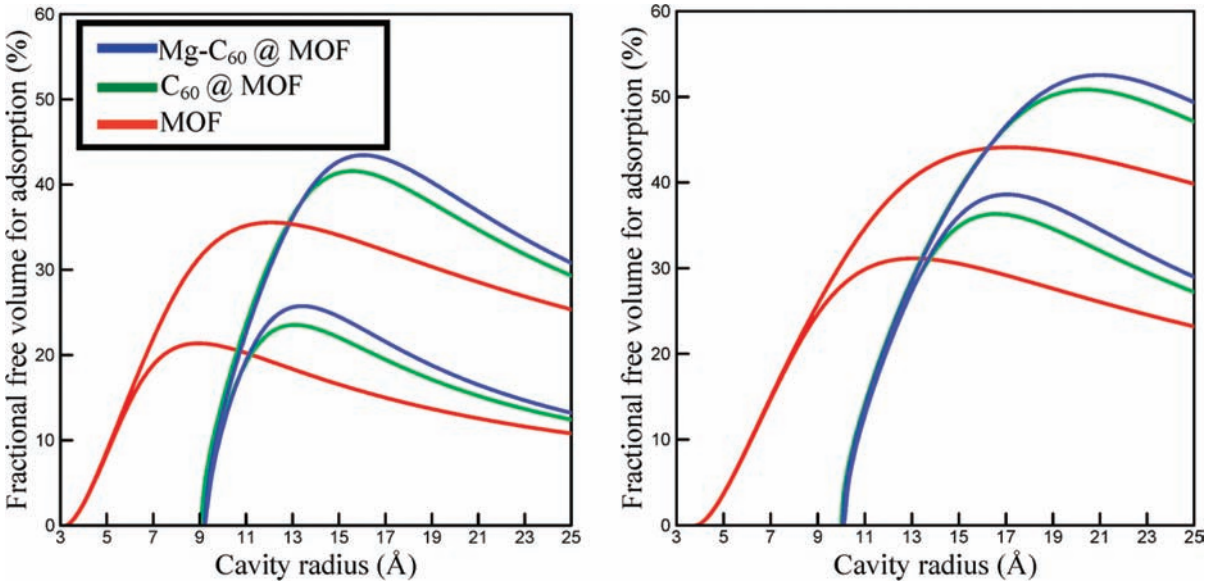

Figure 6. Fractional free volume for adsorption (V_{ad}/V) at 298 K (lower curves) and 77 K (upper curves) for hydrogen (left) and methane (right) as a function of cavity radius r_1.

When r_1 is small (Figure 5A), the overlap of potential energies is strong, and under these conditions the material tends to engender gas adsorption at high enthalpies, but this is offset by a reduction in the free volume that is available for adsorption (Figure 6). Large values of r_1 reduce the potential energy overlap (Figure 5C), but for intermediate r_1 there exists a region where potential energy enhancement can be achieved while still maintaining a substantial free volume (Figure 5B). In all cases, it is clear that **Mg−C$_{60}$@MOF** has a superior performance over **C$_{60}$@MOF** and unfilled MOF.

Fractional free volume for adsorption (V_{ad}/V) is one of the major factors governing gas storage within porous materials, where V is given by $4/3\pi r_1^3$. It represents that proportion of volume within the MOF where gases will exist in the dense adsorbed state, as opposed to the bulk gaseous state. Figure 6 demonstrates that up to 44% of the free volume within **Mg−C$_{60}$@MOF** is able to accommodate both hydrogen and methane in the densely adsorbed state, which is about 10% more than that for empty MOF structures. In the case of both adsorbing gases, the optimal cavity radius increases at lower temperatures (CH_4 17 Å/298 K, 21 Å/77 K; H_2 13 Å/298 K, 16 Å/77 K). This is because at lower temperatures it is possible for gas molecules to be in the adsorbed state at larger distances from the adsorbent's surface, creating multiple adsorption layers, and thus larger cavities are required to reach the optimal capacity.

Tuning the heat of adsorption within hydrogen storage materials represents perhaps one of the greatest challenges facing those concerned with the viability of hydrogen-powered transport. Most physisorbent materials operate well below the 15.1 kJ mol^{-1} proposed as necessary for room temperature operation.[5,22] Since we find that it is possible to overlap surface potential energies through pore impregnation (Figure 6), we expect to see some enhancement in the measured heat of adsorption, as calculated through Van't Hoff plots (Supporting Information) and shown in Figure 7.

The increase in the heat of adsorption observed through the fullerene impregnation is appreciable. Our calculations conservatively predict a heat of adsorption of 11 kJ mol^{-1} for **Mg−C$_{60}$@IRMOF-8**. This value is slightly lower than for very recently reported materials that have heats of adsorption as high as 12.5 kJ mol^{-1} for Cu/Zn mixed metal frameworks[44] or 13.5 kJ mol^{-1} for frameworks with exposed Ni^{2+} sites.[7] However, the heavier metals with a more dense overall structure would be likely to render these materials less capable of significant weight percentage gas uptake. Moreover, the optimum cavity radius is much smaller in these materials, ca. 6 Å, while in the present materials the space available for adsorption of H_2 is much greater and is calculated to be optimum at the much larger r_1 radius of 13 Å (Figure 6). Higher enthalpies for **Mg−C$_{60}$@MOF** would also be attainable at smaller r_1 values, but at the expense of the overall gas uptake capacity. Typically, the heat of adsorption decreases with increased H_2 loading, as weak interactions between hydrogen atoms begin to dominate, but as shown here impregnated MOFs provide the required surface interactions to overcome this problem.

The relative increase in the adsorption heat for methane uptake is even more marked than that for hydrogen, with **Mg−C$_{60}$@MOF** providing an enhancement of more than 100%. As shown in Figure 7, the calculated value, 13.5 kJ mol^{-1}, is close to that required for an ideal methane storage material.[5]

Gas uptake is evaluated from the values of V_{ad} and V_{bulk}, as shown in the Supporting Information. The hydrogen uptake calculated with this method at low pressures as shown in Figure 8 demonstrates substantial enhancement under these conditions, with H_2 uptake as high as 7.6 wt % at just 10 atm for

(38) Panella, B.; Hirscher, M.; Putter, H.; Muller, U. *Adv. Funct. Mater.* **2006**, *16* (4), 520.
(39) Ryan, P.; Broadbelt, L. J.; Snurr, R. Q. *Chem. Commun.* **2008**, (35), 4132.
(40) Kaye, S. S.; Dailly, A.; Yaghi, O. M.; Long, J. R. *J. Am. Chem. Soc.* **2007**, *129* (46), 14176.
(41) See ref 17.
(42) Furukawa, H.; Miller, M. A.; Yaghi, O. M. *J. Mater. Chem.* **2007**, *17* (30), 3197.
(43) Dailly, A.; Vajo, J. J.; Ahn, C. C. *J. Phys. Chem. B* **2006**, *110* (3), 1099.
(44) Chen, B.; Zhao, X.; Putkham, A.; Hong, K.; Lobkovsky, E. B.; Hurtado, E. J.; Fletcher, A. J.; Thomas, K. M. *J. Am. Chem. Soc.* **2008**, *130* (20), 6411.

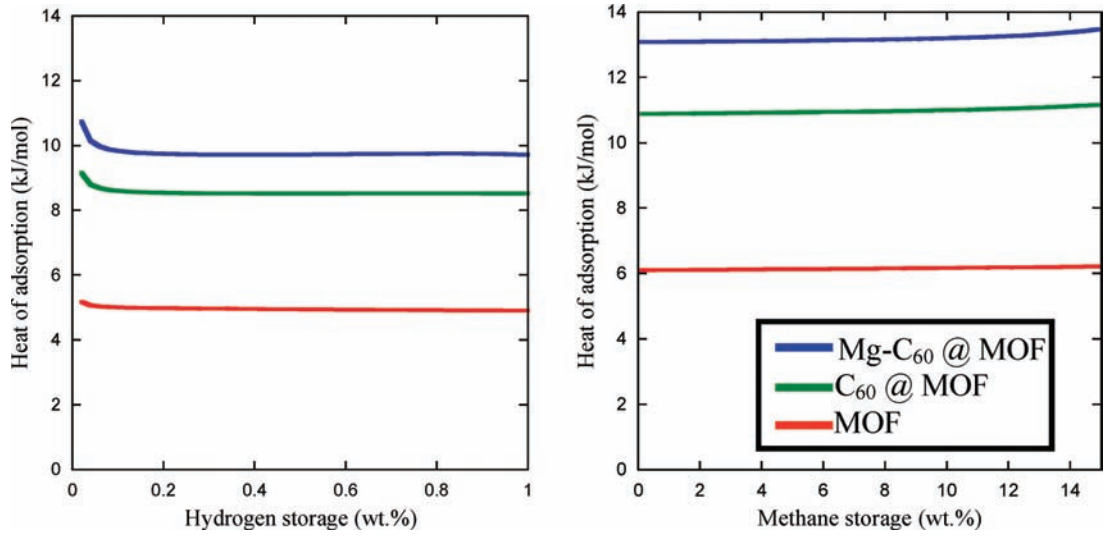

Figure 7. Heat of adsorption within IRMOF-8 for hydrogen (left) and methane (right). IRMOF-8 was chosen for this specific case as the cavity size approaches the optimal value which is determined from Figure 6.

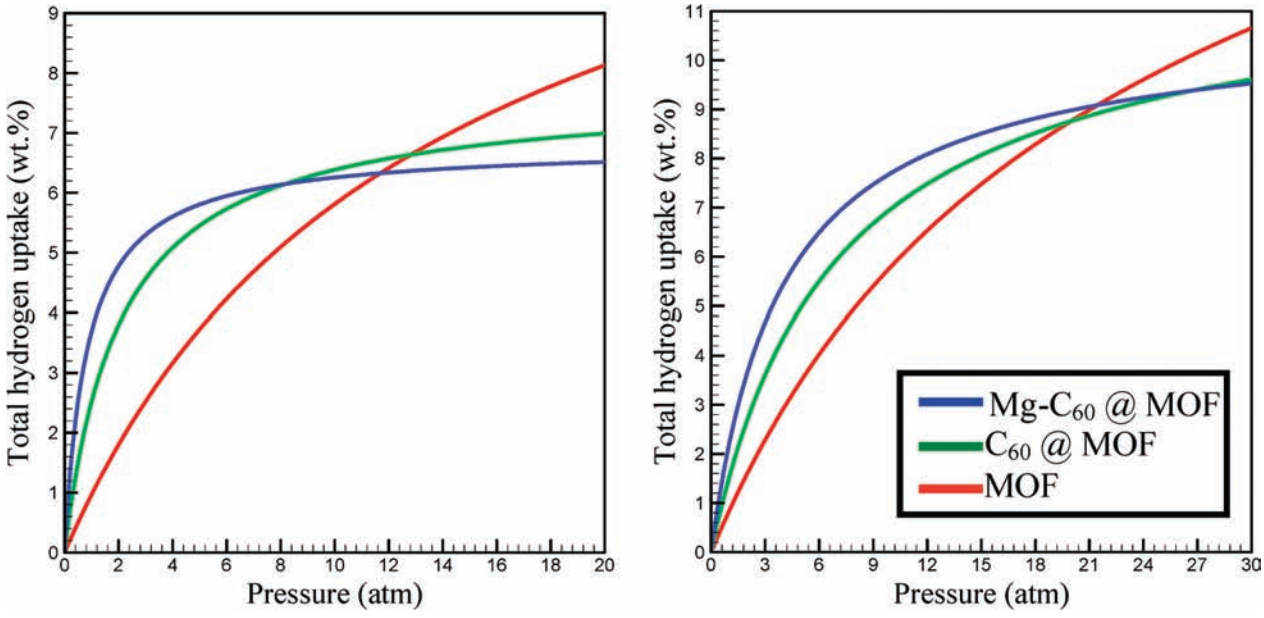

Figure 8. Modeling of total hydrogen storage (wt %) within IRMOF-8 (left) and IRMOF-10 (right) at 77 K.

Mg−C_{60}@MOF-10. Further development of this strategy may remove the need for high pressure vessels.

The effect of fullerene impregnation on methane storage is even more pronounced because of the hydrophobic nature of the fullerene surface. The gravimetric values demonstrated in Figure 9 may be compared to the U.S. DoE volumetric figure of merit of 180 v/v for adsorbed natural gas storage.[15,19] As shown in Figure 10, both bare and decorated fullerenes produce substantial increases in the predicted methane uptake values when impregnated in MOFs. The material **Mg−C_{60}@IRMOF-8** has the highest predicted methane uptake of 265 v/v, presumably due to the increase in hydrophobic groups present.

In assessing the potential viability of such a novel structure, possible limitations to the synthesis have been surveyed. The potential for metal clustering on the fullerene surface has been considered. Kawazoe and co-workers[45] postulated several metal-decorated fullerene structures with varying stabilities. While their modeling predicts $Li_{12}C_{60}$ and $Ca_{32}C_{60}$ to be stable entities, clustering for $Li_{32}C_{60}$, $Mg_{32}C_{60}$, and $Ti_{12}C_{60}$ is also predicted.[46] Yildirim et al.[25] explored stable structures involving Cs-, Ti-, V-, and Cr-decorated fullerenes. As shown in Figure 1, we propose impregnation of MOFs using $Mg_{10}C_{60}$. This relatively low Mg loading would result in Mg atoms being located over phenanthrenate subunits, as opposed to single pentagonal faces seen for more densely loaded fullerenes with up to 32 metal atoms. The closely related Mg anthracenes are known to be particularly stable.[47−54] In light of these predictions and experiments, we believe that $Mg_{10}C_{60}$ is likely to be a stable structure with the Mg atoms well separated.

Another potential challenge with the synthesis and performance of these materials is the possible volatility of fullerenes at reduced pressures. While a bare fullerene may indeed be volatile, a

(45) Sun, Q.; Wang, Q.; Jena, P.; Kawazoe, Y. *J. Am. Chem. Soc.* **2005**, *127* (42), 14582.
(46) Wang, Q.; Sun, Q.; Jena, P.; Kawazoe, Y. *J. Chem. Theory Comput.* **2009**, *5* (2), 374.

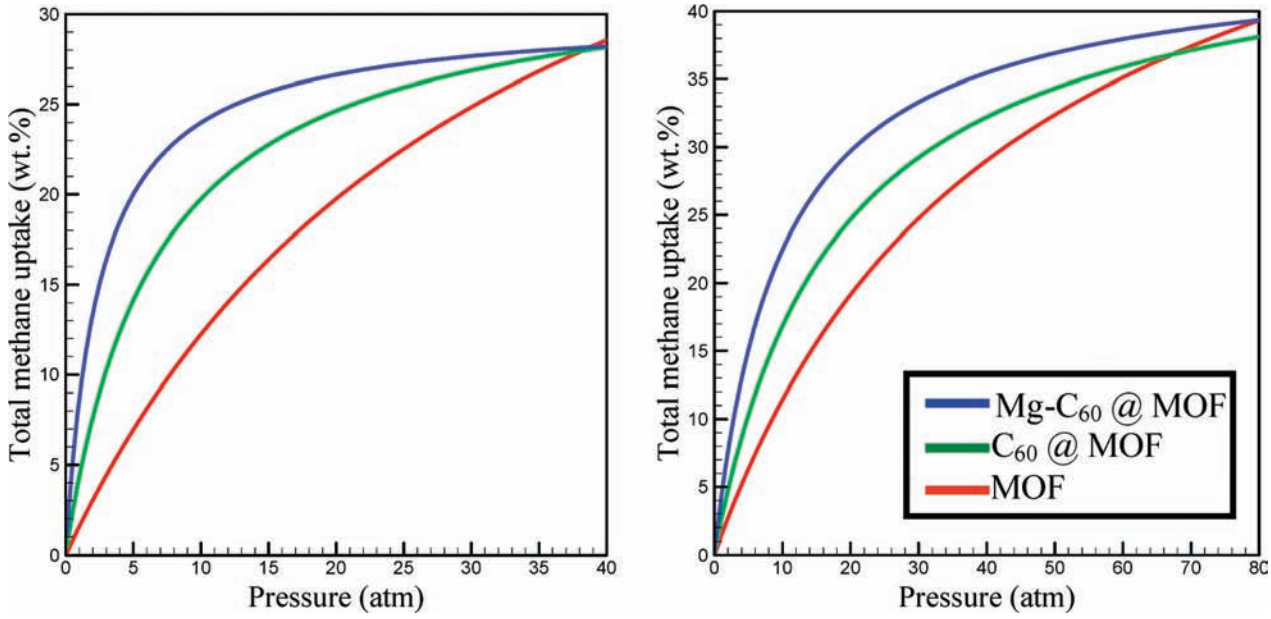

Figure 9. Modeling of total methane uptake (wt %) within IRMOF-8 (left) and IRMOF-10 (right) at 298 K.

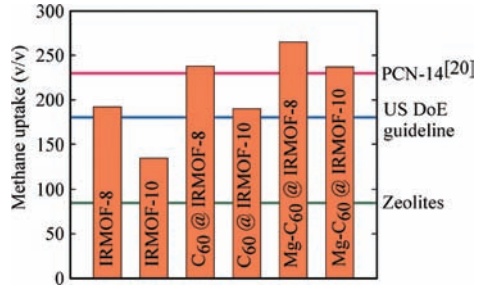

Figure 10. Predicted methane uptake performance for impregnated MOFs at 35 atm and 298 K.

magnesium-decorated fullerene would most likely have a very low vapor pressure. The most active of volatile Mg cluster complexes, typically used as precursors in thin film chemical vapor deposition,[55−58] still require substantially elevated temperatures for evaporation to occur. Coupled with this, the distribution of fullerenes throughout MOF pore channels and their interaction with MOF pore walls would provide further stabilization.[28]

Conclusions

We have described a new concept for hydrogen and methane storage materials, modeling the specific example of magnesium-decorated fullerenes within metal−organic frameworks using a new approach, TIMTAM. Perhaps surprisingly, capacity was found to increase despite an apparent loss of free volume related to pore filling by fullerenes. The increase in capacity was related to the tunability of pore sizes in conjunction with a drastic increase in adsorption enthalpy. The TIMTAM approach was designed to be deliberately conservative to ensure that our results display a high degree of verisimilitude, so that the actual physical materials may possibly display an even higher performance. Moreover, TIMTAM is verified using published experimental results. The predicted properties include methane uptake of 265 v/v, which is the highest reported value for any material, exceeding the U.S. DoE target by a remarkable 47%. In addition, we obtain one of the highest reported physisorption hydrogen adsorption heats of 11 kJ mol^{-1}, which does not diminish with increased hydrogen loading. Effort toward the experimental realization of these materials is ongoing within CSIRO laboratories.

Acknowledgment. A.W.T. acknowledges funding support from the Australian Postgraduate Award, the CSIRO Office of the Chief Executive postgraduate scholarship, and the Australian Research Council. M.R.H. and A.J.H. acknowledge funding support from the CSIRO Science Leader Scheme. We also acknowledge funding support from the CSIRO Energy Transformed Flagship and the Australian Research Council through the Discovery Project Scheme. We thank Ms. Kim Phillips for her kind assistance with the figures.

Supporting Information Available: Further details regarding the parameter values applied for the TIMTAM method and an example of the influence of the location of the fullerene within the pore. This material is available free of charge via the Internet at http://pubs.acs.org.

JA9036302

(47) van den Ancker, T. R.; Harvey, S.; Raston, C. L. *J. Organomet. Chem.* **1995**, *502* (1−2), 35.
(48) van den Ancker, T. R.; Raston, C. L. *Organometallics* **1995**, *14* (2), 584.
(49) Brooks, W. M.; Raston, C. L.; Sue, R. E.; Lincoln, F. J.; McGinnity, J. J. *Organometallics* **1991**, *10* (7), 2098.
(50) Harvey, S.; Junk, P. C.; Raston, C. L.; Salem, G. *J. Org. Chem.* **1988**, *53* (14), 3134.
(51) Harvey, S.; Raston, C. L. *J. Chem. Soc., Chem. Commun.* **1988**, (10), 652.
(52) Engelhardt, L. M.; Harvey, S.; Raston, C. L.; White, A. H. *J. Organomet. Chem.* **1988**, *341* (1−3), 39.
(53) Junk, P. C.; Raston, C. L.; Skelton, B. W.; White, A. H. *J. Chem. Soc., Chem. Commun.* **1987**, (15), 1162.
(54) Raston, C. L.; Salem, G. *J. Chem. Soc., Chem. Commun.* **1984**, (24), 1702.
(55) Hill, M. R.; Russell, J. J.; Lamb, R. N. *Chem. Mater.* **2008**, *20* (7), 2461.
(56) Hill, M. R.; Jensen, P.; Russell, J. J.; Lamb, R. N. *Dalton Trans.* **2008**, (20), 2751.
(57) Hill, M. R.; Lee, E. Y. M.; Russell, J. J.; Wang, Y.; Lamb, R. N. *J. Phys. Chem. B* **2006**, *110* (18), 9236.
(58) Hill, M. R.; Jones, A. W.; Russell, J. J.; Roberts, N. K.; Lamb, R. N. *J. Mater. Chem.* **2004**, *14* (21), 3198.